

*promoting access to White Rose research papers*



**Universities of Leeds, Sheffield and York**  
**<http://eprints.whiterose.ac.uk/>**

---

This is an author produced version of a paper published in **Polymer**.

White Rose Research Online URL for this paper:

<http://eprints.whiterose.ac.uk/10274>

---

**Published paper**

Tomlinson, M.R., Cousin, F., Geoghegan, M. (2009) *Creation of dense polymer brush layers by the controlled deposition of an amphiphilic responsive comb polymer*, *Polymer*, 50 (20), pp. 4829-4836

<http://dx.doi.org/10.1016/j.polymer.2009.05.021>

---

# Creation of dense polymer brush layers by the controlled deposition of an amphiphilic responsive comb polymer

Michael R. Tomlinson<sup>1\*</sup>, Fabrice Cousin<sup>2</sup>, and Mark Geoghegan<sup>1</sup>

<sup>1</sup> Department of Physics and Astronomy, The University of Sheffield, Sheffield S3 7RH, UK

<sup>2</sup> Laboratoire Léon Brillouin CEA/CNRS UMR12, CE-Saclay, F-91191 Gif-sur-Yvette Cédex, France

We introduce a copolymer with a comb topology that has been engineered to assemble in a brush configuration at an air-water interface. The molecule comprises a 6.1 kDa poly(methyl methacrylate) backbone with a statistical amount of poly[2-(dimethyl amino)ethyl methacrylate] polybase side chains averaging 2.43 per backbone. Brush layers deposited with the hydrophobic PMMA backbone adsorbed to hydrophobized silicon are stable in water even when stored at pH values less than 2.0 for over 24 h. The use of a Langmuir trough allows a simple controlled deposition of the layers at a variety of grafting densities. Depth profiling of brush layers was performed using neutron reflectometry and reveals a significant shifting of the responsiveness of the layer upon changing the grafting density. The degree of swelling of the layers at a pH value of 4 (below the  $pK_b$ ) decreases as grafting density increases. Lowering the pH of the subphase during deposition causes the side chains to become charged and more hydrophilic extending to a brush-like configuration while at neutral pH the side chains lie in a “pancake” conformation at the interface.

Keywords: combs, brushes, stars, PMMA, poly[2-(dimethyl amino)ethyl methacrylate], neutron reflectometry

## 1. Introduction

The modification of surfaces with polymer chains has received a lot of attention recently. Polymers tethered to surfaces function in a variety of capacities including biocompatibilization, responsive surfaces, lubrication, and prevention of fouling. The study of weak polyelectrolytes at surfaces is of particular interest due to their responsive nature. Applications of polyelectrolyte brushes are now starting to appear [1, 2], and possible applications of temperature-responsive brushes [3, 4], are also likely.

There are two ways to permanently modify surfaces with tethered polymer chains, each having distinct advantages [5, 6]. The first, the “grafting to” approach, involves synthesizing a polymer with a functional end group that may be used to covalently bind the polymer chains to a reactive surface. In

PMMA backbone PDMAEMA side chains

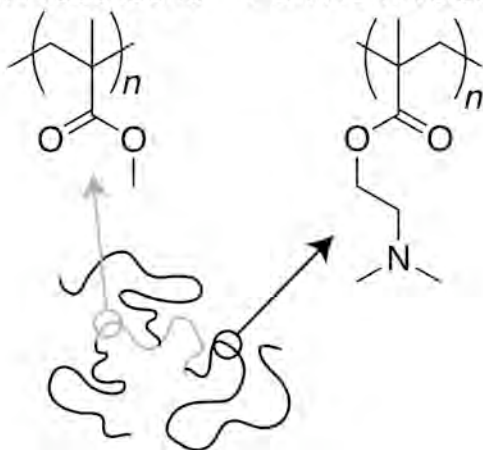


**Fig. 1.** The copolymer material synthesized is composed of PMMA backbones (grey) with a statistical numbers of PDMAEMA side chains (black) averaging 2.43 side chains per backbone. Due to the random multi-arm nature of this polymer the overall polydispersity is quite large, however, the polydispersity of the side chains should be low.

this method, the polymer chains may be synthesized with precise characterization of molecular weight ( $M_n$ ) and polydispersity index so that the chains at the surface are well known. The density of grafted chains is, however, limited sterically by the radius of gyration of the polymer chain. Thus, the “grafting to” layers are also limited in thickness due to the small amount of adsorbed material.

The second route to a tethered polymer layer, the “grafting from” method, involves using an initiator-modified substrate along with a controlled polymerization technique to grow chains directly from the surface. Post-characterization of polymer layers proves to be a time-consuming and difficult task as the layers must either be cleaved and

\* m.tomlinson@alumni.ncsu.edu

analyzed with size exclusion chromatography (SEC) [7] or characterized in the film with a technique like single molecule force spectroscopy [8-10]. The “grafting from” method typically creates highly dense layers on the order of 0.5 chains/nm<sup>2</sup> [11]. Also, these films may be grown to much greater thicknesses due to the low steric hindrance of individual monomer molecules as opposed to the large polymer chains used in the “grafting to” method. Normally, the grafting density depends on the density of the initiator layer and the conditions of the polymerization. Some methods that have been used to vary the grafting density include mixing monolayers of active/inactive initiator molecules [7, 9], partial degradation of the full initiator layer before polymerization [12], and LB deposition of the initiator layer [11], or simply control of the time taken for the adsorption of the initiator monolayer [13]. These methods are very stable but are specific only to substrates on which the silane or thiol initiator will self assemble. They also use harsh chemicals, and can vary in their predictability.

Ideally, one may wish to create a well-characterized polymer brush layer with precise molecular weight, polydispersity, and grafting density. In this work we consider a possible route towards polymer brush synthesis which involves a specialized “grafting to” method using a Langmuir trough along with a comb copolymer which has the ability to self organize into a brush configuration. With this method, we are able to pre-characterize the polymer and adjust the grafting density and thickness of the layer simply by adjusting the deposition area on the Langmuir trough.

The polymer molecule is an amphiphilic comb polymer with a poly(methyl methacrylate) (PMMA) backbone and sparsely grafted responsive poly[2-(dimethyl amino)ethyl methacrylate] (PDMAEMA) side chains (Fig. 1). The polymer backbone and side chains are synthesized in two separate atom transfer radical polymerization (ATRP) [14] steps. In some circumstances it is as well to consider the polymer, PMMA-*graft*-PDMAEMA, as a star polymer, because the size of the side chains is substantially larger than the hydrophobic PMMA backbone, which may then be treated as a rather bulky multifunctional site from which the arms extend. PDMAEMA, a polybase, typically charges at acidic pH with a pK<sub>b</sub> in solution between 7 and 8 [15]. Preliminary evidence suggests that these films are responsive to changes in pH and may be tuned by adjusting the density of grafted chains as well as the environmental pH at time of deposition.

## 2. Experimental Section

### 2.1 Materials

Methyl methacrylate (MMA) (99%, Aldrich), 2-hydroxyethyl methacrylate (HEMA) (98%, Aldrich), 2-(dimethyl amino)ethyl methacrylate (DMAEMA) (98%, Aldrich), CuCl<sub>2</sub> (> 99%, Aldrich), ethyl- $\alpha$ -bromoisobutyrate (98%, Aldrich), anhydrous diethyl ether (Fisher), anhydrous dichloromethane (DCM, Fisher), triethylamine (TEA) (99%, Aldrich), 4-(dimethyl amino)pyridine (DMAP) (99%, Aldrich),  $\alpha$ -bromoisobutyryl bromide (99%, Aldrich) were all used as received. CuCl (> 99%, Aldrich) was sequentially rinsed with 10% aqueous HCl, methanol, and diethyl ether, before drying in vacuum.

### 2.2 ATRP Synthesis of the MMA/HEMA random copolymer backbone

To a nitrogen flushed 100 ml flask 0.307 g (1.96 mmol) bipyridine, 0.093 g (0.936 mmol) CuCl, and 0.0063 g (0.0467 mmol) CuCl<sub>2</sub> was added. 10.0 ml (0.17 mol) ethanol, 10.0 ml (93.5 mmol) methyl methacrylate, and 570  $\mu$ l (4.67 mmol) hydroxyethyl methacrylate were added

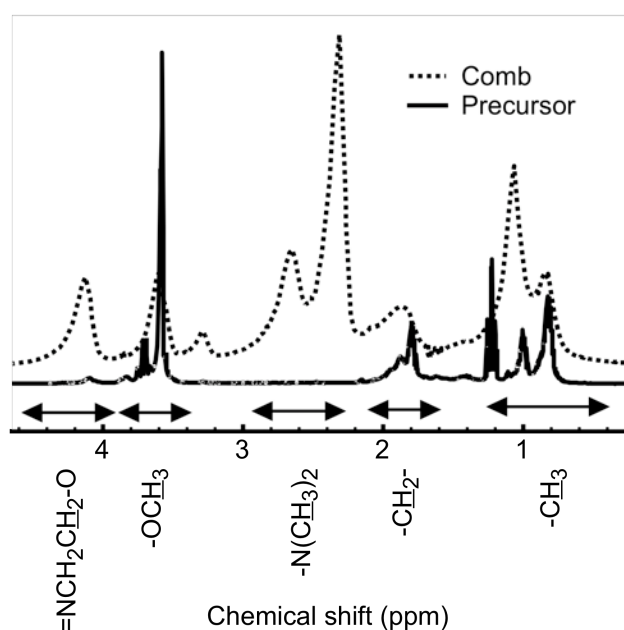


**Fig. 2.** <sup>1</sup>H NMR spectra of PMMA-*co*-PHEMA precursor and PMMA-*graft*-PDMAEMA.

sequentially after being sparged with nitrogen for 10 min each. After all solids were dissolved and a dark homogeneous solution was achieved, 92  $\mu\text{l}$  (0.623 mmol) of ethyl-2-bromoisobutyrate was added. The vial was sealed and allowed to react for 24 h at 25°C. The polymerization was stopped at less than 40% conversion to ensure a random copolymerization with no intramolecular gradients.

The solution was injected through a syringe packed with silica gel until a colourless liquid was obtained. The polymer was precipitated into hexane, redissolved in acetone, precipitated again into hexane, and dried under vacuum for two days.

$^1\text{H-NMR}$  was performed in deuterated chloroform. Hydrogen peaks (at 3.82 ppm and 4.10 ppm) corresponding to the HEMA unit were observed (Fig. 2). These HEMA peaks (less the contribution due to the ethyl- $\alpha$ -bromoisobutyrate  $-\text{OCH}_2-$  peak) were compared with the backbone hydrogen peaks (at a chemical shift of 0.8-1.1 ppm) and indicated that the polymer was composed of 4.6% HEMA units.

SEC was performed in tetrahydrofuran (THF) against PMMA standards. The  $M_n$  and polydispersity index of the backbone came to 6.1 kDa (61 repeat units) and 1.17 respectively.

### 2.3 Chemical modification of backbone to ATRP macroinitiator

To 10 ml anhydrous DCM, 1 g of poly(MMA-*co*-HEMA) polymer was added. 200  $\mu\text{l}$  TEA and 200  $\mu\text{l}$  DMAP were added to the mixture. 200  $\mu\text{l}$  bromoisobutyryl bromide was added dropwise to the mixture and all was left undisturbed for 24 hours. The solution was twice rinsed with 0.1M HCl, and then twice with 0.1M NaCl. The solution was allowed to sit over molecular sieves to remove residual water, before drying under vacuum.

$^1\text{H-NMR}$  performed in deuterated chloroform indicated the presence of the bromoisobutyryl group (at 1.96 ppm) and a shifting of the characteristic HEMA peaks (to 3.82 ppm, 4.10-4.20 ppm, and 4.37 ppm). These shifts confirmed the chemical modification of the HEMA sites to bromoisobutyryl-initiating sites. The bromoisobutyryl peak indicated that there were 3.7% bromine-terminated initiating sites per backbone repeat units. Residual chlorine termination (2.15 ppm) from the backbone polymerization must also be added because the backbone terminations are also viable initiating sites. Only 18% of the chains retained the original chlorine termination so the total chlorine and bromine-initiating sites came to 4.0% of the total backbone repeat units. From this we estimate that each chain has an average of 2.43 viable initiating sites out of 61 repeat units. The bromoisobutyryl peak (1.96 ppm) was not visible in the final spectrum of the comb polymer.

### 2.4 Synthesis of PMMA-graft-PDMAEMA comb copolymer

24.1 mg CuCl and 54  $\mu\text{l}$  PMDETA were added to a 50 ml flask purging with nitrogen. 2.14 ml ethanol, and 2.14 ml DMAEMA monomer were added to the flask after each was sparged with nitrogen for 10 min. To another smaller flask, 0.0521 g of the poly(MMA-*co*-HEMA) macroinitiator, 2.2 mg CuCl<sub>2</sub>, and 400  $\mu\text{l}$  acetone (sparged with nitrogen) were added. After both solutions were homogeneous the contents of the smaller flask were transferred to the 50 ml flask initiating the reaction. The flask was left sealed for 24 h.

The content of the flask was diluted with 15 ml of ethanol and run through a syringe filled with silica gel. Once the copper was removed the solution was precipitated in alkaline water (pH 10) at 40°C. The polymer was collected and dried under vacuum.

### 2.5 $^1\text{H-NMR}$ characterization of comb polymer

$^1\text{H-NMR}$  of the comb polymer (Fig. 2) revealed that the ratio of DMAEMA to PMMA (taken from  $\text{N}=(\text{CH}_2)_2$  at 2.25-2.30 ppm and  $-\text{O}-\text{CH}_3$  at 3.52 ppm) yields an average comb  $M_n = 127.0$  kDa. Assuming 2.43 side chains per backbone (from initiating sites) implies an average side chain  $M_n = 49.8$  kDa or 317 repeat units.

### 2.6 SEC characterization with molecular weight modelling.

The gel permeation chromatography (GPC) setup comprised two Polymer Laboratories PL gel 5  $\mu\text{m}$  MIXED-C columns. The GPC eluent was HPLC grade THF containing 2.0 % (v/v) TEA and 0.05% (w/v) BHT (2,6-di-*tert*-butyl-(4-methylphenol)) at a flow rate of 1.0 ml/min. The column temperature was set at 30°C. Ten near-monodisperse PMMA standards ( $M_n = 2$ -300 kDa) were used for

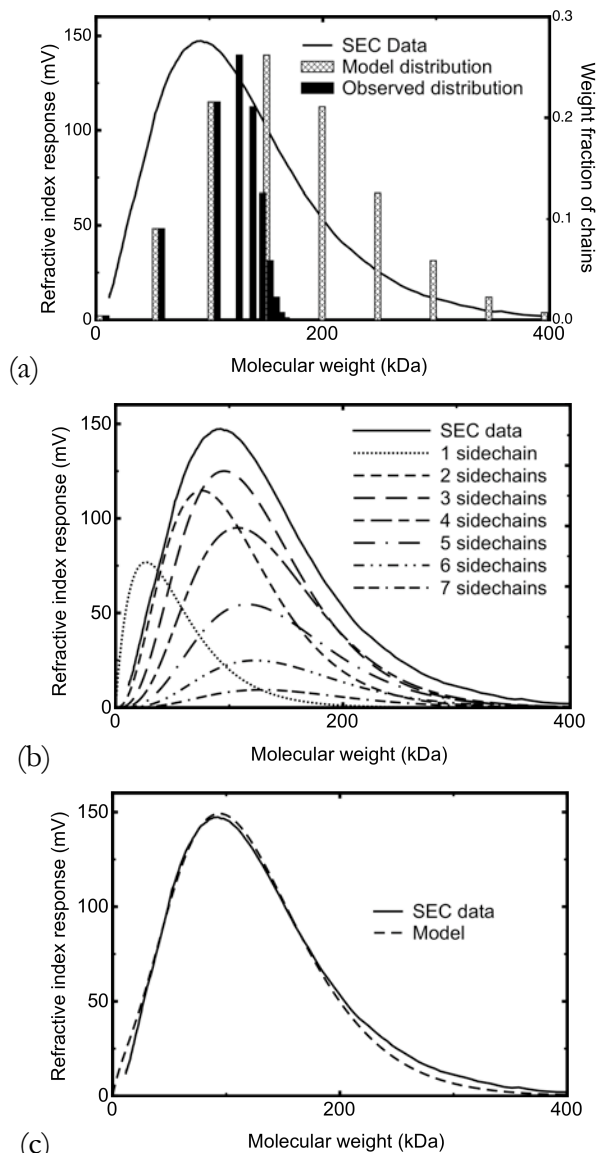


**Fig. 3.** (a) Comb polymer SEC refractive index response distribution (solid line) shown with “model” distribution of  $M_n$  averages calculated with equations 1 & 2 (light bars) and the “observed” distribution of averages corresponding to  $M_n$ 's as would be observed by SEC on an  $M_n$  scale made with linear polymer standards translated via equation 5 (dark bars). The data for the SEC distribution are the “observed” molecular weights, based on SEC calibration. (b) Expansions of observed averages for combs of various numbers of side chains from 1-7 calculated with equation 6 (dotted lines) added together to approximate the model SEC distribution (solid line) also shown in (a). (c) The “model signal” curve is produced by the summation of all seven curves from (b). As illustrated, this model curve provides a very good approximation to the SEC data.

backbone chains with a functionality  $f$ .  $f_f$  is equal to the number of combinations of  $f$  initiating units in a group composed of  $N_b$  units multiplied by the probability,  $a$ , of having  $f$  initiating units and  $N_b - f$  non-initiating units,

$$f_f = \frac{N_b!}{f!(N_b - f)!} a^f (1 - a)^{(N_b - f)}. \quad (1)$$

We also know, from  $^1\text{H-NMR}$ , the average molecular weight of each of the side chains ( $M_{n,s} = 49.8$  kDa). The final molecular weight  $M_{n,f}$  ( $M_n$  of the  $f$ -armed comb) is given by

calibration. The data were analyzed using PL Cirrus GPC software (version 2.0) supplied by Polymer Laboratories.

As SEC is a characterization technique built upon the separation of chains of different size and thermodynamic characteristics (not molecular mass), polymer chains with complex architectures and topologies generally cannot be characterized using SEC with polymer standards. More often, polymers with non-linear architectures are characterized with SEC columns in combination with a variety of detectors. Detector setups that are available include multi-angle laser light scattering (MALLS), viscometric, as well as traditional refractive index (RI). When using a multi-detector it is usually possible to obtain absolute values for  $M_n$  and polydispersity, assuming accurate values of the specific refractive index ( $dn/dc$ ), appropriate detector constants, and sufficient detector signal-to-noise ratios.

In this work, we use an alternative technique by developing a model of the comb polymer consistent with the observed molecular weight distribution obtained from SEC against polymer standards. Note that it is incorrect to estimate molecular weight of non-linear polymer chains by comparing with SEC of linear standards because SEC is based on molecular *size* and not molecular *mass*. The results of this model agree well with the predicted  $M_n$  from  $^1\text{H-NMR}$  and are consistent with the total length at full chain extension gathered from the neutron reflectometry (NR) measurements. Using this method we are able to characterize the comb polymer by simple SEC against standards with an accuracy that could accompany triple-detection characterization in the future.

To begin to model the distribution we must first obtain the statistical distribution of  $f$ -functionalized backbone chains. We can use a combination function along with the known fraction of initiating monomer units ( $a = 0.040$  from  $^1\text{H-NMR}$ ) and the number average degree of polymerization ( $N_b$ ) of the backbone to derive an equation for the fraction  $f_f$  of

$$M_{n,f} = M_{n,b} + fM_{n,s}. \quad (2)$$

Using equations 1 and 2 we can now calculate a model  $M_{n,f}$  distribution of the combs. This distribution may be seen in Fig. 3a.

In order to compare the modelled polymer distribution to SEC data, we must translate the model  $M_{n,f}$  data (knowing molecular weight and functionality number) to match the scale of the linear polymer standards. The radius of gyration ( $R_g$ ) is a simple parameter to describe the size of a chain and can be relatively easily modelled for both linear and more complex chains [16]. As mentioned in the introduction, we can treat this molecule as an  $f$ -arm star due to the relatively small size of the backbone. The radius of gyration of an  $f$ -arm star polymer is easily estimated, and so we consider that here [17]. The radius of gyration of a linear polymer ( $R_{g,L}$ ) and a star polymer ( $R_{g,s}$ ) can be modelled as follows,

$$\langle R_{g,L} \rangle^2 = \frac{N_L^{2\nu} b^2}{6} \quad (3)$$

and

$$\langle R_{g,s} \rangle^2 = P(f) \left( \frac{N_s^{2\nu}}{f} \right) \frac{b^2}{6} \left( 3 - \frac{2}{f} \right), \quad (4)$$

where  $b$  is the monomer Kuhn length,  $N_L$  and  $N_s$  are the degree of polymerization of the linear and star respectively ( $N_s/f$  is the molecular mass of each branch),  $\nu$  is the Flory exponent which is 0.59 for a good solvent, and  $P(f)$  is a prefactor dependent on the number of arms. For small values of  $f$ , we can assume  $P(f)$  is close to unity [18]. If we set these radii equal and solve for  $N_L$  (which is therefore the number of monomers in a linear chain required to give an equivalent size to that of the star polymer) we obtain an equation, which relates the observed SEC molecular mass (that of a linear polymer) to the actual molar mass of a star polymer.

$$N_L = N_s \left( \frac{3 - \frac{2}{f}}{f} \right)^{1/2\nu} \quad \text{or} \quad M_{n,L} = M_{n,f} \left( \frac{3 - \frac{2}{f}}{f} \right)^{1/2\nu} \quad (5)$$

Finally, we take the  $M_{n,f}$  values and expand each average value into a model polydisperse distribution. Polymer distributions, including those of stars and combs, have been successfully modelled using a Schulz-Zimm distribution [19-21]. The Schulz-Zimm function is a gamma probability distribution tailored to describe polydispersity,

$$g(N_n, \alpha, \beta) = N_n^{\alpha-1} \frac{\beta^\alpha e^{-\beta N_n}}{\Gamma(\alpha)}, \quad (6)$$

where  $\alpha = N_{av}/\beta$ ,  $\beta = \sigma^2/N_{av}$  ( $N_{av}$  is the average degree of polymerization),  $N_n$  is the degree of

**Table 1** Estimation of backbone and side chains  $M_n$  and polydispersity (PDI). The observed molecular weight from SEC is much less than actual  $M_n$  due to the smaller molecular size of the comb polymer compared to a linear chain.

|                | $M_n$ (PDI) backbone | $M_n$ (PDI) side chain | $M_n$ (PDI) total |
|----------------|----------------------|------------------------|-------------------|
| NMR            | 5.8 kDa              | 49.8 kDa               | 127.0 kDa         |
| SEC (observed) | 6.1 kDa (1.17)       |                        | 86.4 kDa (1.41)   |
| SEC (model)    |                      | 54.9kDa (1.51)         | 126.6 kDa (1.58)  |

polymerization, and  $\sigma^2$  is the variance of the distribution. The expanded set of distributions is shown in Fig. 3b. The addition of these curves produces the model curve which is shown along with the SEC curve in Fig. 3c. The final result of this fit suggests that the comb has an average of 2.43 chains per backbone with each chain having a molecular weight of 49 kDa. A summary of  $M_n$  and polydispersity values obtained by <sup>1</sup>H-NMR, SEC, and modelling is shown in Table 1.

### 3. Results and Discussion

#### 3.1 Preparation of Langmuir-Blodgett (LB) and Langmuir-Schäfer (LS) films from comb copolymer at various grafting densities and their characterization by scanning force microscopy (SFM).

The polymer was dissolved in chloroform (methylene chloride produced identical films) at a concentration of 0.66 mg/ml. This solution was spread over an air-water interface in a Langmuir trough and allowed to equilibrate for 15 minutes. The barrier speed was set at 30 cm<sup>2</sup>/min. PDMAEMA, having amphiphilic monomers, is able to form isotherms even without a hydrophobic backbone, so we can assume that, at low coverage, it forms a two-dimensional monolayer arrangement on the air/water interface. A compression isotherm of surface pressure vs. molecular area over deionized water can be seen in Fig. 4a.

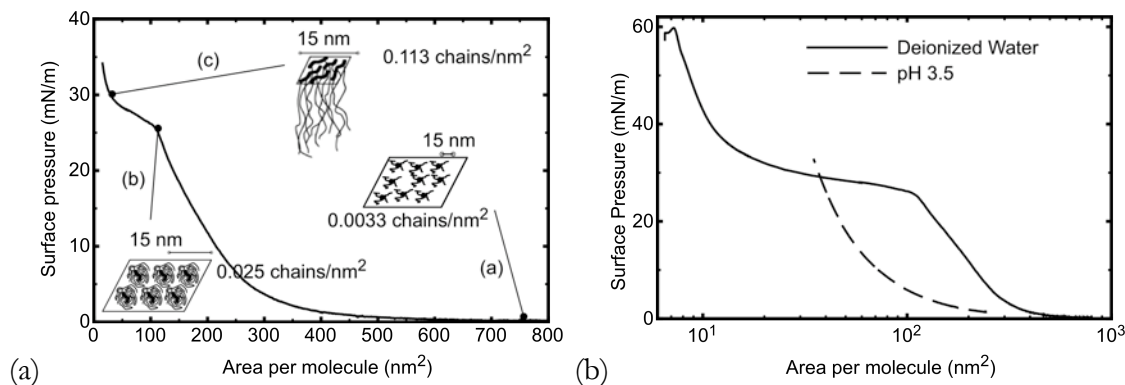


**Fig. 4.** (a) Surface pressure isotherms of comb film deposited over neutral subphase pH. The molecular conformation at low medium and high surface pressures is shown in the three cartoons. (b) As the subphase becomes more acidic the three regions collapse to a single inclined curve bypassing the plateau region, presumably because the side chains are sufficiently charged that they no longer anchor to the interface. Note also that the acidic incline occurs at a much lower grafting density, possibly due to a charged or salted brush effect, which increases the effective chain diameter.

Before discussing the isotherm in Figs 4a and 4b it is helpful to estimate the radius of gyration ( $R_g$ ) of a single side chain. Here we use the Flory equation with an appropriate prefactor (0.23-0.24 has been used for polydimethylsiloxane and polystyrene [22, 23], and seem reasonable here) for a DMAEMA monomer and an exponent of 0.59 for a good solvent, so we have  $R_g \approx 0.24N_0^{0.59} = 7.1$  nm (where  $N_0 = N_s/f$ ), and so  $R_g^2 \approx 50$  nm<sup>2</sup> per chain. Considering that there are 2.4 chains per backbone, the area per molecule where the swollen side chains should begin the transition from mushroom to brush conformation should be approximately from  $2.4R_g^2$  to  $2.4\pi R_g^2$  or between  $2.4 \times 50$  nm<sup>2</sup> = 120 nm<sup>2</sup> and  $2.4 \times 3.14 \times 50$  nm<sup>2</sup> = 376 nm<sup>2</sup> per molecule. (We note that 2.4 arms per chain is a relatively low side chain grafting density and so we expect there to be no interference between the individual branches as has been anticipated using Monte Carlo simulations [18].) If the side chains and backbone are behaving as a three-dimensional expanded coil exhibiting a mushroom to brush transition, then the region of transition should start at approximately 120 to 376 nm<sup>2</sup> per molecule.

Indeed, the onset of increasing surface pressure occurs in this mushroom-brush transition region. However, we postulate that a pancake to brush transition is actually occurring here. Upon examining the deionized H<sub>2</sub>O isotherm, we can divide the data into four distinct regions (Fig. 4a). The first region, found at molecular areas of approximately 310 nm<sup>2</sup> or greater, corresponds to a molecular diameter of greater than 20 nm. In this region, the polymer is spread at a low concentration on the water surface; both the hydrophobic backbone and the uncharged amphiphilic side chains lie flat on the surface extended and avoiding contact with neighbouring molecules.

In the second region from approximately 110 nm<sup>2</sup> to 310 nm<sup>2</sup>, individual molecules begin to feel the presence of other neighbouring chains. Though still lying flat on the surface, the chains begin to be compressed closer to one another. It is likely that, in this region, neighbouring chains start to interpenetrate significantly.

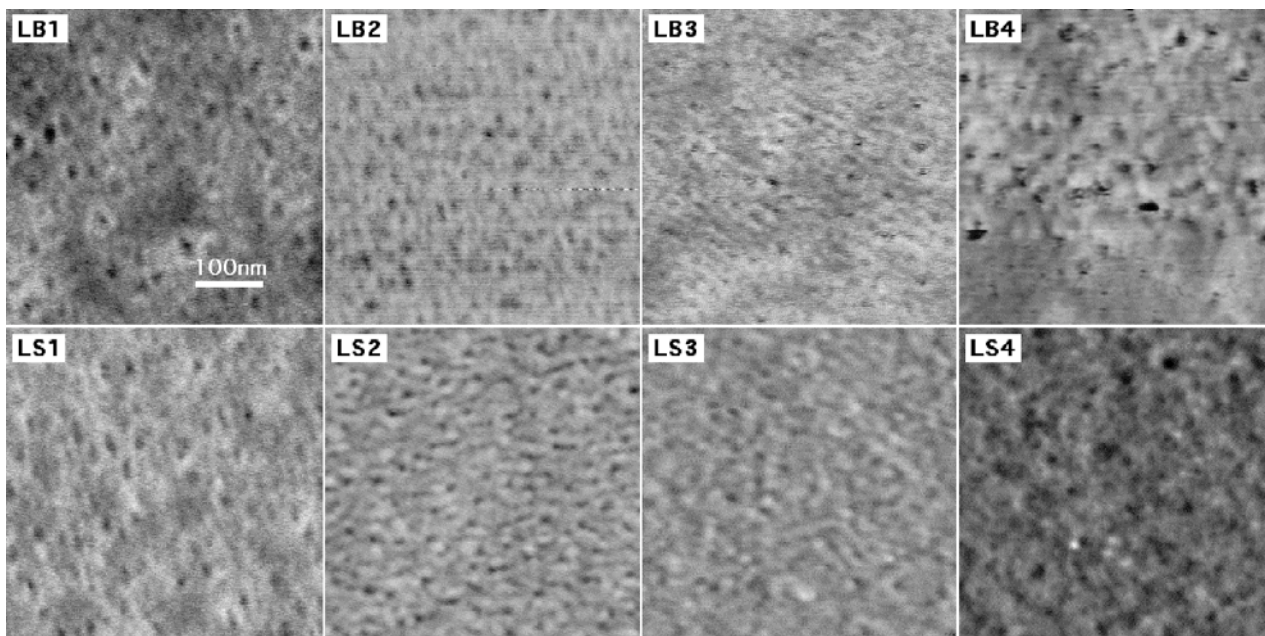


**Fig. 5.** SFM images of LS and LB films deposited on a silicon surface. The surface pressures of deposition are 21 (LB1, LS1), 23 (LB2, LS2), 26 (LB3, LS3) and 32 (LB4, LS4) mN/m. The size of the features (pores) closely matches molecular size. These features disappear as the film becomes flatter in LS films.

At the beginning of the third region ( $\sim 110 \text{ nm}^2$ ), we suggest that the chains have been compressed close enough so that all monomer units can no longer all remain in a monolayer at the surface. This phenomenon was also observed in non-electrolytic systems and the semi-plateau corresponding with this transition was dubbed the “pancake region” in which part of each molecule is submerged in order to relieve the increasing pressure [24]. The argument for a “pancake” region as opposed to a submerged mushroom region seems valid since PDMAEMA without a PMMA backbone exhibits the semi-plateau region as well meaning that the amphiphilic PDMAEMA chains can partially anchor to the surface without the need of a hydrophobic backbone. This theory seems to be validated by the corresponding area per monomer unit of  $0.135 \text{ nm}^2$  of the beginning of this plateau region. This area seems low compared with values obtained for PMMA; however, we believe this occurs due to the fact that PDMAEMA monomers orient with the long hydrophilic side group facing into the subphase, thus reducing the surface area. Films deposited from the plateau region (discussed below) reveal only molecular rearrangement in regular unit cells matching the area/molecule predicted by the isotherm.

The fourth and final region ( $< 50 \text{ nm}^2$ ) shows a marked increase in the work required to decrease the surface area. A PDMAEMA homopolymer spread in the same way exhibits all of the regions except this final one, demonstrating that the sharp increase in surface pressure at low molecular area is due to backbone proximity. Additionally, a comparison of the pressure increase in this region as a function of grafting density reveals that the curve does not fit any known scaling laws [25] of a mushroom to brush transition. It is not clear, however, how much of this pressure occurs because the PMMA backbones come close enough to each other to begin packing side-by-side or because the side chains, anchored to the interface via the backbones, begin to enter the brush regime. It is likely that a combination of these two phenomena is happening. Further compression results in a time-dependent loss of surface pressure that cannot be regained by a decompression/recompression cycle, probably indicating that some of the PMMA backbones are submerged with the possible formation of micelles which would prevent a return to surface-confinement.

The fact that the side chains of the comb are a weak polybase enables us to change the subphase pH and observe how the isotherm is affected. Fig. 4b shows the original deionized water isotherm along with an isotherm compressed over water at pH 3.5 (well below the  $\text{pK}_b$ ). At this pH, the chains should be charged and extended into the solution. The first difference we observe is that the “pancake” region discussed above disappears completely, indicating that the monomers in this region are no longer in a monolayer on the surface. The second major difference is that the brush regime occurs at much higher molecular areas indicating that the charged chains (coordinating with water) occupy a higher molecular volume than the uncharged chains. This comparison supports the presence of a pancake conformation at the semi-plateau and a brush regime in the final region of increasing surface pressure.

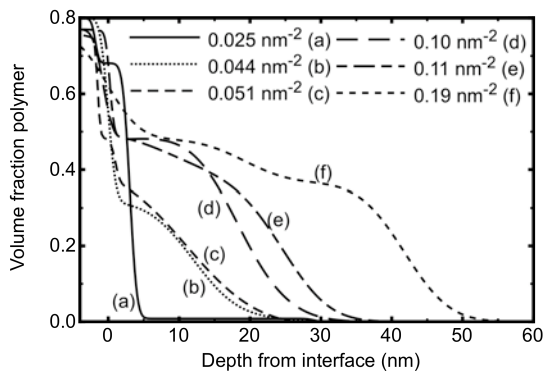


**Fig. 6.** Volume fraction-depth profiles of several LS films that were created and the profiles measured in  $D_2O$  at pH 8.0 for different surface pressures. These results indicate that the pressure at which these films were deposited is directly related to the polymer density at the interface, which ranges from 40% to 65% volume fraction. Note that at the air-water interface, the volume fraction never reaches unity demonstrating that perfect packing is not achieved.

molecules as being around 130 kDa. Some research into creating dense layers via amphiphilic copolymer LB assembly has been performed in the past [26-35], but we have shown that multi-molecular micellation (creating structures  $> 100$  nm) has been largely prevented through controlling polymer chain architecture. Such films could potentially be used as ultrathin size-selective nanofiltration films for sensor applications, templates for nanolithography, or an environmentally acceptable way to tune the physical and chemical properties of a flat surface.

### 3.2 Neutron reflectometry determination of polymer surface density-depth profiles

NR measurements were performed on the time-of-flight EROS reflectometer using the Orphée reactor at the Laboratoire Léon Brillouin. LS layers were deposited at a variety of conditions onto a hydrophobized 5 cm diameter circular silicon wafer of 4 mm thickness. In order to avoid the problem of air bubbles interfering the brush-water interface, specialized liquid cells were used to keep the wafer in contact with a solution of a given pH. Using this cell, the neutrons travelled through the silicon substrate from below (a geometry not available on many reflectometers), which prohibited the interface of interest from being contaminated with air bubbles.  $D_2O$ , with its large scattering length density, was used in place of  $H_2O$  to provide contrast with the hydrated polymer layer. The layers, once deposited, were very stable in water even at  $pH < 2$ , although the layer could be forcibly removed by rinsing while the layer was charged. Care was taken to neutralize the layer by injecting pH 10 water into the cell before removing the sample from the aqueous environment. All fits to the NR data were made using the *slab fit* routine [36] where the density profile is assumed to be described adequately as the sum of up to 20 uniform layers of material (though more than 4 layers were seldom needed) and three Gaussian roughness parameters: one each for the outer and innermost interfaces, and the third for all the internal ones. During each of the fits, the polymer composition is conserved to within 5% error. This free-form fitting routine is optimized using a downhill simplex routine by increasing the number of layers until a satisfactory fit is found. In the present work,

A series of LB and LS depositions were performed on silicon surfaces at the specific locations along the deionized water isotherm. Essentially, layers deposited via LS deposition can be thought of as “brush-side-up” since the hydrophobic backbone comes in contact with the silicon surface first, while layers deposited via LB will tend to be “backbone-side-up.” The explanation offered for the plateau and high-pressure region is supported by SFM images taken from these samples (Fig. 5). However we believe that, due to only moderate hydrophilicity, the side chains adopt only a partial brush-like configuration.

Based on the SFM images, we believe that the molecules remain isolated from one another creating patterns only on the size scale of the individual molecules (5-20nm). In fact, the size of features in the SFM images matches exactly with the calculated area/molecule deposited with the LB trough further supporting an average molecular weight of the comb

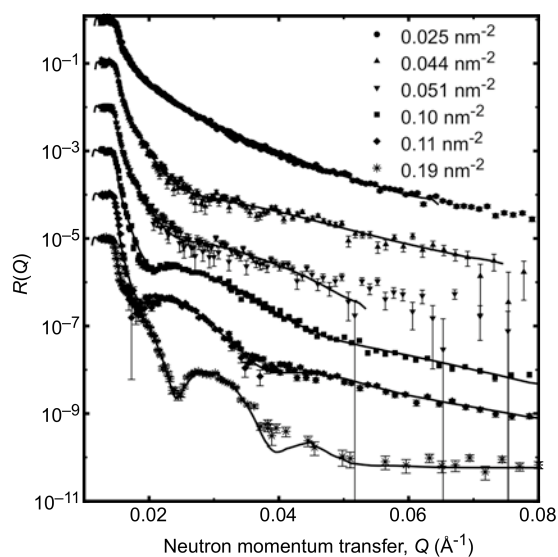


**Fig. 7.** Neutron reflectometry data and fits of brush samples at pH 8.0 (deionized  $D_2O$ ) with  $\chi^2 < 1.0$  for different surface densities from 0.025 to 0.19 polymers/nm<sup>2</sup>.

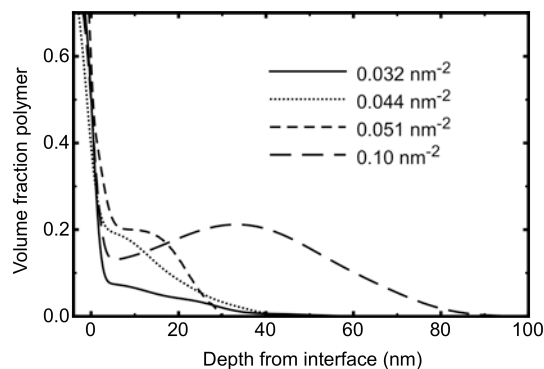


**Fig. 8.** Volume fraction-depth profiles for several LS films that were created and the profiles (at different polymer surface densities) measured in D<sub>2</sub>O at pD 4.0. Though all films are swollen, the centre of polymer density moves away from the surface as the pD is lowered.

and 0.10 chains per nm<sup>2</sup> (corresponding to between 50 and 25 nm<sup>2</sup> per molecule). Somewhere below a grafting density of 0.10 chains/nm<sup>2</sup> the polymer volume fraction reaches a maximum of approximately 48%. Simultaneously, the maximum thickness of the layer begins to increase from a constant value of approximately 20 nm to nearly 50 nm. The contour length of one side chain, assuming a monomer unit length of 0.25 nm<sup>2</sup>, should be approximately 87 nm, while the radius of gyration, as estimated earlier, is assumed to be on the order of 50 nm<sup>2</sup>.

Fits for the reflectivity data corresponding to the brushes at pD 8 are shown in Fig. 7. Here, the quality of the fits is excellent with  $\chi^2 < 1$ . At pD 4 (Fig. 8), the densest brush stretches the most, as expected. The monotonic decay of the brushes with distance from the substrate is observed for all of the samples, except for the densest (0.10 chains/nm<sup>2</sup>), a phenomenon observed in our previous work on polybase brushes synthesized using an ATRP *grafting from* method [1, 36], and possibly explained by the effect of greater charge towards the free end of the chains [37]. The NR fits for the pD 4 condition all have  $\chi^2 < 2$ .

As we have seen above, the effect of charging can affect the volume fraction-depth profile of the brush, but it can also affect the point at which the brush starts to swell. We have noted above that the pK<sub>b</sub> for PDMAEMA is between 7 and 8 in dilute solution. If we consider a brush of 0.04 chains/nm<sup>2</sup> as a function of pH, we note a dramatic increase in swelling as the pH is lowered below 4 (Fig. 9). The change in pK<sub>b</sub> is due to the confinement of the polyelectrolyte layer. PDMAEMA chains with monomer units less than one Bjerrum length apart will be affected by counterion condensation, which lowers the effective pK<sub>b</sub> of the system.

## 4. Conclusions

We have shown that amphiphilic comb polymers form good quality brush layers when assembled and compressed using a Langmuir trough. After deposition, the layers are stable and adhere to a hydrophobized silicon dioxide interface even at pH < 2 where the polybase side chains should be highly charged. The grafting density of these polymers may be tuned simply by adjusting the compression of the layers in the Langmuir trough. Layers produced at higher grafting densities exhibit a denser, less responsive layer as shown by NR measurements.

The pH of the subphase during deposition plays an important role in creating a more compact brush. Deposition when the molecules are relatively neutral (pH > 7) leads to profiles that are densest near the surface and monotonically decrease into the solution phase, whereas if the chains are too

all fits were good with normalized  $\chi^2 < 3$  in all cases.

The NR experiments were performed on samples at different deposition surface pressures and as a function of pH. A number of conclusions can be made from these experiments. At pD 8 (we use pD because deuterated water is used for NR), the brush is expected to be mostly collapsed and so the thickness of the brush layer is expected to be proportional to the grafting density. Changes in conformation of the brush as a function of grafting density mean that this conclusion is difficult to test quantitatively, probably because PDMAEMA remains soluble in water at high pH, but at pD 8 (Fig. 6) it is clear that the brush is behaving as expected in this respect. It is also clear that a transition occurs between grafting densities of 0.05

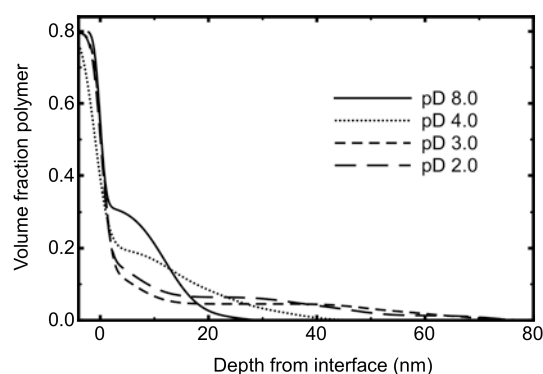


**Fig. 9.** Volume fraction-depth profiles for single LS film in D<sub>2</sub>O at various pD. As pD decreases (more acidic), the polymer charges and extends into solution.

charged at acidic pH and at reasonably high grafting density the layers exhibited a maximum in the polymer density 15-20 nm away from the wafer interface. Using this method we are able to self assemble well-characterized brush layers onto a generally hydrophobic surface.

**Acknowledgment.** We acknowledge financial support from the European Community's "Marie-Curie Actions" under contract MRTN-CT-2004-504052 [POLYFILM]. This research project has been supported by the European Commission under the 6th Framework Programme through the Key Action: Strengthening the European Research Area, Research Infrastructures. Contract n°: RII3-CT-2003-505925. We thank Sasha Heriot for helping with the Langmuir trough, and Tim Richardson for its use.

## References

1. La Spina R, Tomlinson MR, Ruiz-Pérez L, Chiche A, Langridge S, and Geoghegan M. *Angew. Chem. Int. Ed.* 2007;46:6460-6463.
2. Zhou F, Shu W, Welland ME, and Huck WTS. *J. Am. Chem. Soc.* 2006;128:5326-5327.
3. Collett J, Crawford A, Hatton PV, Geoghegan M, and Rimmer S. *J. R. Soc. Interface* 2007;4:117-126.
4. Kaholek M, Lee W-K, Ahn S-J, Ma H, Caster KC, LaMattina B, and Zauscher S. *Chem. Mater.* 2004;16:3688-3696.
5. Rühle J. Polymer brushes: On the way to tailor-made surfaces. In: Advincula R, Brittain WJ, Caster KC, and Rühle J, editors. *Polymer brushes: synthesis, characterization, applications.* Weinheim: Wiley-VCH, 2004. pp. 1-31.
6. Zhao B and Brittain WJ. *Prog. Polym. Sci.* 2000;25:677-710.
7. Jones DM, Brown AA, and Huck WTS. *Langmuir* 2002;18:1265-1269.
8. Goodman D, Kizhakkedathu JN, and Brooks DE. *Langmuir* 2004;20:6238-6245.
9. Parnell AJ, Martin SJ, Dang CC, Geoghegan M, Jones RAL, Crook CJ, Howse JR, and Ryan AJ. *Polymer* 2009;50:1005-1014.
10. Yamamoto S, Tsujii Y, and Fukuda T. *Macromolecules* 2000;33:5995-5998.
11. Devaux C, Cousin F, Beyou E, and Chapel J-P. *Macromolecules* 2005;38:4296-4300.
12. Yamamoto S, Ejaz M, Tsujii Y, and Fukuda T. *Macromolecules* 2000;33:5608-5612.
13. Topham PD, Howse JR, Crook CJ, Parnell AJ, Geoghegan M, Jones RAL, and Ryan AJ. *Polym. Int.* 2006;55:808-815.
14. Patten TE and Matyjaszewski K. *Adv. Mater.* 1998;10:901-915.
15. Bütün V, Armes SP, and Billingham NC. *Polymer* 2001;42:5993-6008.
16. Rubinstein M and Colby RH. *Polymer Physics.* Oxford: Oxford University Press, 2003.
17. Zimm BH and Stockmayer WH. *J. Chem. Phys.* 1949;17:1301-1314.
18. Whittington SG, Kosmas MK, and Gaunt DS. *J. Phys. A: Math. Gen.* 1988;21:4211-4216.
19. Gu L, Zhu S, and Hrymak AN. *J. Polym. Sci. B: Polym. Phys.* 1998;36:705-714.
20. Shiau L-D. *Polymer* 2002;43:2835-2843.
21. Zhu S, Li D, Yu Q, and Hunkeler D. *J. Macromol. Sci. A: Pure Appl. Chem.* 1998;35:33-56.
22. Fetters LJ, Hadjichristidis N, Lindner JS, and Mays JW. *J. Phys. Chem. Ref. Data* 1994;23:619-640.
23. Lapp A, Picot C, and Benoit H. *Macromolecules* 1985;18:2437-2441.
24. da Silva AMG, Filipe EJM, d'Oliveira JMR, and Martinho JMG. *Langmuir* 1996;12:6547-6553.
25. Kent MS, Lee LT, Factor BJ, Rondelez F, and Smith GS. *J. Chem. Phys.* 1995;103:2320-2342.
26. Baker SM, Leach KA, Devereaux CE, and Gragson DE. *Macromolecules* 2000;33:5432-5436.
27. Cheyne RB and Moffitt MG. *Langmuir* 2005;21:5453-5460.
28. Chung B, Choi M, Ree M, Jung JC, Zin WC, and Chang T. *Macromolecules* 2006;9:684-689.
29. Currie EPK, Sieval AB, Avena M, Zuilhof H, Sudhölter EJR, and Cohen Stuart MA. *Langmuir* 1999;15:7116-7118.
30. Francis R, Skolnik AM, Carino SR, Logan JL, Underhill RS, Angot S, Taton D, Gnanou Y, and Duran RS. *Macromolecules* 2002;35:6483-6485.
31. Hayashi S, Abe T, Higashi N, Niwa M, and Kurihara K. *Langmuir* 2002;18:3932-3944.
32. Kim Y, Pyun J, Fréchet JMJ, Hawker CJ, and Frank CW. *Langmuir* 2005;21:10444-10458.
33. Mouri E, Matsumoto K, Matsuoka H, and Torikai N. *Langmuir* 2005;21:1840-1847.
34. Seo Y, Paeng K, and Park S. *Macromolecules* 2001;34:8735-8744.
35. Shin K, Rafailovich MH, Sokolov J, Chang DM, Cox JK, Lennox RB, Eisenberg A, Gibaud A, Huang J, Hsu SL, and Satija SK. *Langmuir* 2001;17:4955-4961.
36. Geoghegan M, Ruiz-Pérez L, Dang CC, Parnell AJ, Martin SJ, Howse JR, Jones RAL, Golestanian R, Topham PD, Crook CJ, Ryan AJ, Sivia DS, Webster JRP, and Menelle A. *Soft Matter* 2006;2:1076-1080.
37. von Goeler F and Muthukumar M. *Macromolecules* 1995;28:6608-6617.